EXPERIMENTAL AND NUMERICAL EVALUATION ON THE HELICOPTER ROTOR RESPONSE UNDER THE CRASH IMPACT

Changbae Lee, Seoul, Seoul National University (Korea, Republic of)
Kunhyuk Kong, Seoul, Seoul National University (Korea, Republic of)
Seung-Hoon Kang, Seoul, Seoul National University (Korea, Republic of)
Minho Hwang, Seoul, Seoul National University (Korea, Republic of)
SangJoon Shin, Seoul, Seoul National University (Korea, Republic of)

Abstract

When the helicopter rotor collides, the relevant impact load on the blade will be transmitted to the fuselage though its hub. In this paper, collision analysis of the rotor blades under hard impact is conducted by both experimental and numerical approach. To obtain reliable test results, the collision of the rotating blades will be simulated by drop and whirl tower tests. UH-60A main rotor blade is selected and designed for each experiment. For the drop situation, the maximum indentation during the crash impact is evaluated experimentally and numerically using ANSYS LS-DYNA. In addition, the behavior of the rotor blade and the tendency of an impact force in terms of time and displacement under 2 drop tests are compared. Finally, the rotor blade and hub design of Mach-scaled UH-60 rotor blade is conducted for the whirl tower tests. In the future, the whirl tower test will be conducted for hover of both 4-blade and one-blade-out condition at Seoul National University Rotor Test Stand (SNURTS). The loads acting on the hub are measured and correlated against those predicted numerically.

1. INTRODUCTION

Helicopter crash may cause catastrophic damage on the vehicle component, and directly affects the crew survivability. Therefore, analyzing the consequence of the crash impact will be crucial for ensuring the safety of the helicopter and crew. To address this issue, MIL-STD 1290A[1] has been established to achieve the desirable crash resistance capability. Park, et al.[2] performed drop test and numerical analysis on the crash resistance of the composite lower fuselage based on the impact speed presented in MIL-STD 1290A. Furthermore, many rotorcraft crash tests and numerical analyses conducted by NASA[3] were reported in the literatures. U.S. Army[4] established new criteria for designing a desirable crashworthy rotorcraft. Recent studies were conducted to understand the impact behavior of the airframe and landing gear[5, 6]. However, relatively few studies were conducted on its rotor blade impact. The collision scenarios were limited to be soft such as bird strike, water and wood impact[7, 8]. Rotorcraft also operates in a harsh maritime environment such as the landing on ship deck and the possibility of hard impact will increase[9]. In this paper, hard impact crash of the rotor blades against a rigid object will be analyzed by both experimental and numerical approach. To analyze the crash impact, both whirl tower and drop tests are attempted. UH-60A main rotor blade is selected and the design procedure of the rotor blade for each experiment purpose are proposed. Drop tests are conducted to evaluate the impact force and maximum indentation of the blade damage under the crash impact. In addition, the numerical evaluation is conducted by ANSYS LS-DYNA[10] and the results are compared and discussed between the experimental evaluation. Furthermore, Mach-scaled rotor blade and hub design is conducted for the whirl tower test. In the future, whirl tower test will be conducted to evaluate the load transferred momentarily to the hub.

2. APPROACH FOR ROTOR BLADE CRASH ANALYSIS

When the rotor blades collide, the impact load will be transferred to the hub momentarily. However, it is not quite clear to obtain reliable experimental result consistently from the rotating blade impact. Therefore, in order to analyze such event, both whirl tower and drop tests will be conducted. Whirl tower tests are conducted to analyze the interaction between the load on the blade and the hub. In addition, the drop tests are conducted to analyze the impact load or energy acted upon the rotor blade and the response of the component. To simulate the crash impact, UH-60A main rotor blade is selected. The specifications of it are summarized in Table 1 and Fig. 1.

Table 1: Properties of UH-60A main rotor blade

Property	Value
Number of the blades	4
Type	Articulated
Radius	26.83 ft
Nominal Chord	20.76 in
Nominal RPM	258 rpm
Airfoils	SC1095 / SC1094R8

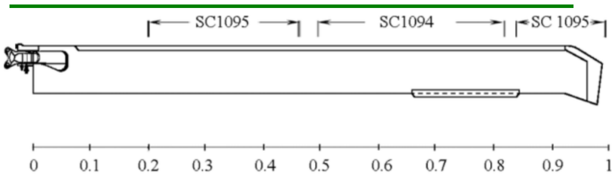

Figure 1: Schematic of UH-60A main rotor blade[11]

3. ROTOR BLADE DROP TEST

3.1. Rotor blade design

The detailed collision situation is defined in MIL-STD 1290A regarding the outer 10% of the main rotor blade span colliding with a rigid cylinder. Furthermore, the outer 10% of the blade span, which is SC1095 airfoil section, is selected as the design point of the present drop test.

UH-60A main rotor blade is composed of E-glass laminate, titanium spar, filled with honeycomb core in the trailing edge, and foam core in the leading edge. The cross section of the rotor blade is shown in Fig. 2.

Figure 2: Cross section of UH-60A rotor blade[12]

To simulate a crash impact realistically, reverse design of UH-60A main rotor blade is conducted to give correct characteristics by using the configuration and experimental results described in Ref. 13. VABS program[14,15] is used to evaluate its flapwise, lagwise, and torsional stiffnesses. Furthermore, an iterative genetic algorithm-sequential quadratic programming (GA-SQP) algorithm in MATLAB is used to correlate the discrepancies on the sectional stiffness against the experimental result to be smaller than a certain tolerance. The presently designed cross section and the stiffnesses of the rotor blade are included in Fig. 3 and Table 2, respectively.

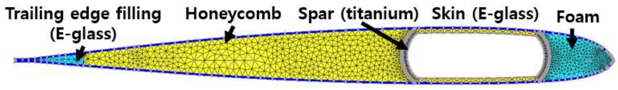

Figure 3: Presently designed rotor blade cross section for the drop test

Table 2: Stiffness of the present rotor blade

Property $[N \cdot m^2]$	EI_{flap}	EI_{lag}	GJ
Experiment[12]	6.4x10^4	2.4x10^6	7.0x10^4
Present	6.2x10^4	2.4x10^6	7.2x10^4
Discrepancy	3.4%	3.0%	0.33%

3.2. Preparation for drop tests

The present rotor blades are fabricated with the fixtures included at both ends and the bottom of the designed test section using E-glass. The fixtures are filled with E-glass contrary to the rotor blade which have hollow titanium spar. Therefore, the fixtures at both ends are designed to cover some portion of the blade and connect each other to avoid inappropriate damage at the discontinuous cross sections during impact. Furthermore, the length of the blade is designed to have negligible effect on the fixture at both ends during the crash impact. The schematic of the blade-fixture assembly is shown in Fig. 4. Accordingly, 2 test specimens are fabricated for drop tests as shown in Fig. 5.

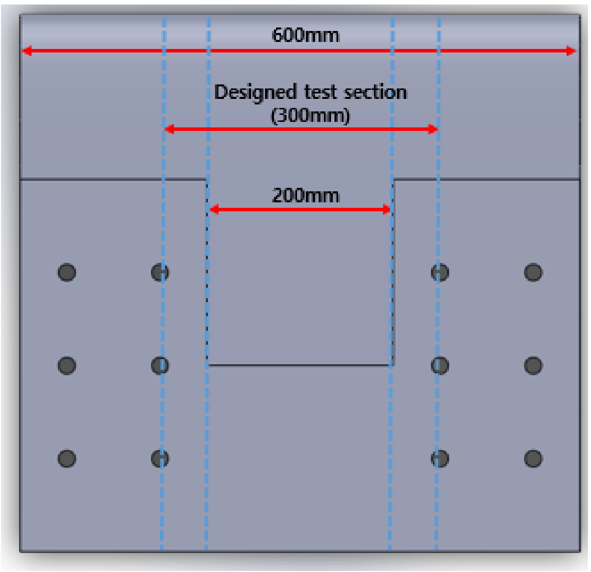

Figure 4: Schematic of the blade-fixture assembly

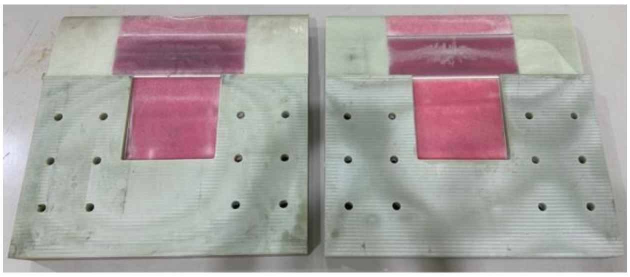

Figure 5: Fabricated blade-fixture assembly

The rigid cylinder is fabricated to be 8 inch in diameter as defined in MIL-STD 1290A and the length of 1.5 times the thickness of the blade to avoid an inappropriate vibration induced into the blade. Furthermore, the cylinder will be comprised of SCM440, which has similar material properties as those of the structural steel. Additionally, the cylinder is assembled with a guide arm and a load cell to be constrained with two poles at both ends to allow only drop in the vertical direction. The assembled impactor is shown in Fig. 6.

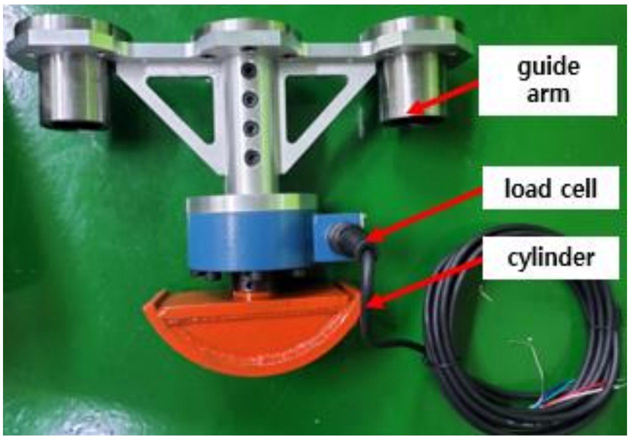

Figure 6: Impactor assembly

The rotor blade is fixed with 4 jigs at the front and back of both ends. The impact load and indentation during the crash impact are measured using the load cell and displacement sensor. Consequently, the impact energy is evaluated. Additionally, the response of the rotor blade under crash impact is evaluated using 2 high speed cameras in the front and back of the rotor blade. The setups for drop tests are shown in Fig. 7.

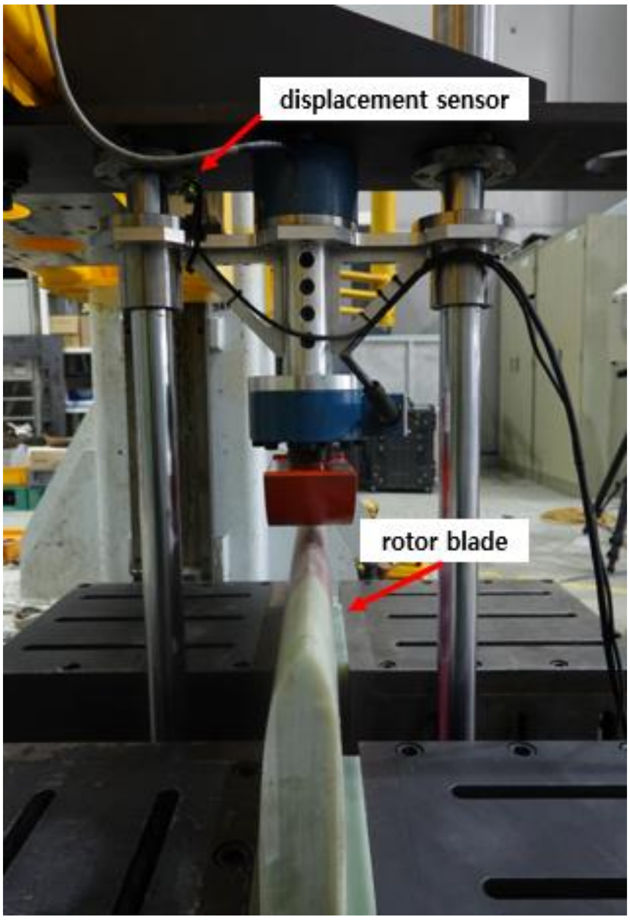

Figure 7: Setups for drop test

3.3. Numerical evaluation

The crash impact is numerically evaluated using ANSYS LS-DYNA, an explicit nonlinear structural finite element analysis software. Figure 8 shows the finite element (FE) representation of the cylinder assembly and the rotor blade. The rotor blade is constructed as described in Sec. 3.1. The skin and spar component consist of shell elements, and all the other components of the blade and the impactor consist of solid elements. Based on the CAD drawing produced by CATIA V5 and ANSYS Designmodeler, the mesh is generated using ANSYS Mechanical with a target mesh size of 10mm. The total mass of the impactor assembly in numerical analysis is set to be identical with that of the measured one. Structural steel is used for the cylinder, and aluminum properties are applied to the other components of the impactor. In addition, impactor is assumed to be rigid, since it is expected to have no significant plastic strain or indentation induced on the cylinder. Since the rotor blade consists of the composite material, Chang-Chang failure criteria (MAT022) will be employed. It is suitable for simulating the progressive failure of each failure mode of the orthotropic material. Any individual element that satisfies the criterion will be eliminated from the analysis. The boundary condition of the blade is set to be fixed where the E-glass fixtures are fabricated and the cylinder assembly is set to move freely only in the vertical direction to satisfy the test condition described in Sec. 3.2. The finite element representation of the impactor consists of 3,006 elements and 4,882 nodes, and the blade consists of 19,670 elements and 14,626 nodes. Furthermore, an interaction between the cylinder and the blade is implemented by using the penalty method as the node-to-surface contact. The duration of the analysis is 0.02s so that the behavior under the impact can be well captured. Finally, the impact velocity of 5.42m/s and gravitational force is applied to the cylinder via the body load function. As a result, maximum indentation of 20.67mm is expected where the impact occurs. Figure 9 shows the deformed blade when the maximum indentation under the crash impact occurs.

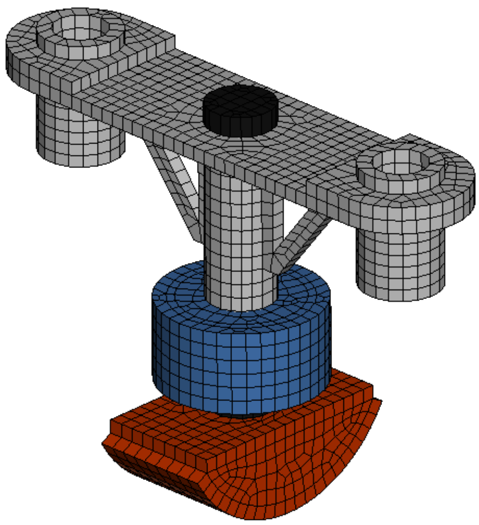

(a) Finite element representation of the impactor

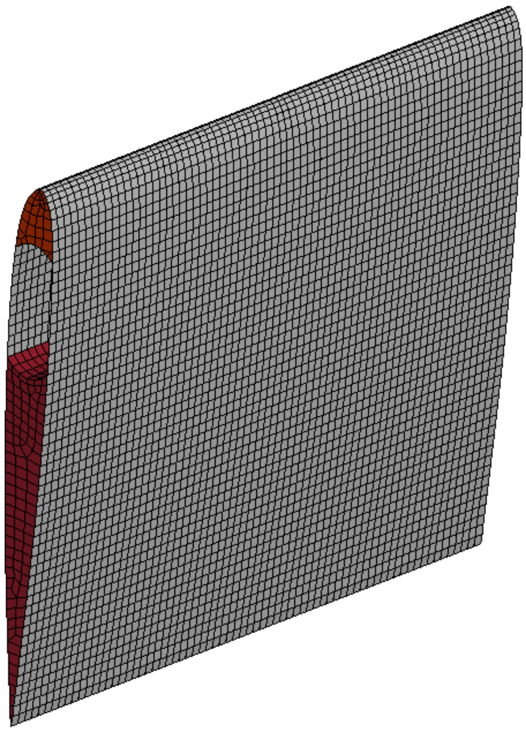

(b) Finite element representation of the blade

Figure 8: FE representation of the impactor assembly and rotor blade for the crash analysis

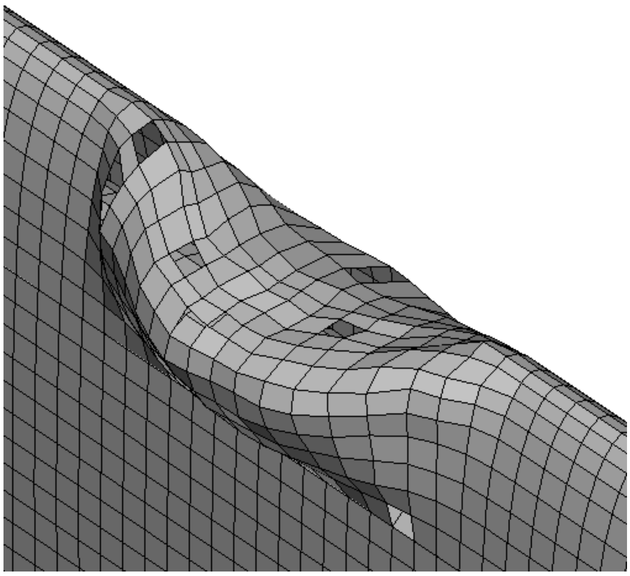

Figure 9: Deformed blade skin under crash impact

3.4. Experimental evaluation

The crash impact is experimentally conducted using the drop test facility shown in Fig. 10. The drop height is set as 1.5m from the leading edge from the rotor blade. Furthermore, 2 drop tests are conducted and the maximum indentation analyzed numerically is compared with the test results. However, load cell measures the upper part of the impactor assembly, which is assumed to be 60% of the total weight. Therefore, impact force and impact energy are only compared between the test results and discussed in this paper.

Figure 10: Rotor blade before drop test

The rotor blades during maximum indentation are shown in Fig. 11. The test results of maximum indentation were 18.8mm and 16.6mm each. In addition, the discrepancies between numerical analysis and the experiments are 9.9% and 24.5%, respectively. The damage from the crash impact did not reach the titanium spar as shown in the numerical analysis. Foam core which is filled between skin and spar absorbed large amount of the impact energy. In consequence, elastic behavior is observed on the impacted area and as the cylinder bounces up, the rotor blades tend to keep in shape. However, the impacted skin is severely damaged. The airfoil of the designed rotor blade for drop tests is SC1095, which is unsymmetrical airfoil. Therefore, different damage mechanisms are observed between the upper and lower surface. Wave shaped lines which are major fiber breakage occurs on the lower surface of the first test specimen and the upper surface of the first and second test specimens. On the contrary, large extent of damages including delamination and fiber breakage are observed across the impacted area of the lower surface skin of the second specimen. The damages on the rotor blades after drop tests are shown in Fig. 12.

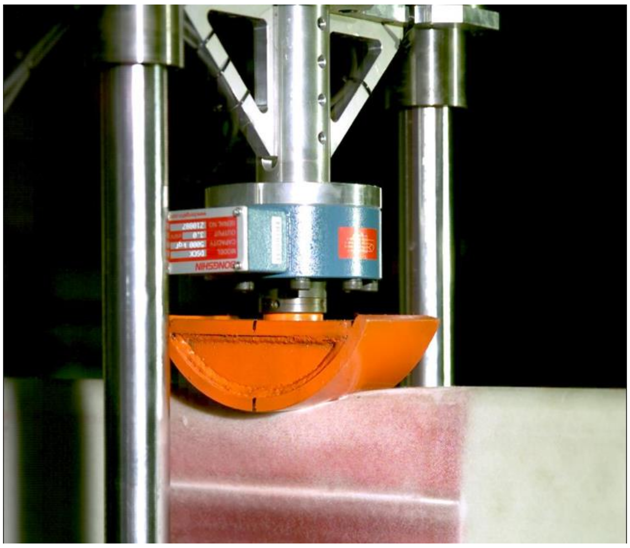

(a) First test specimen

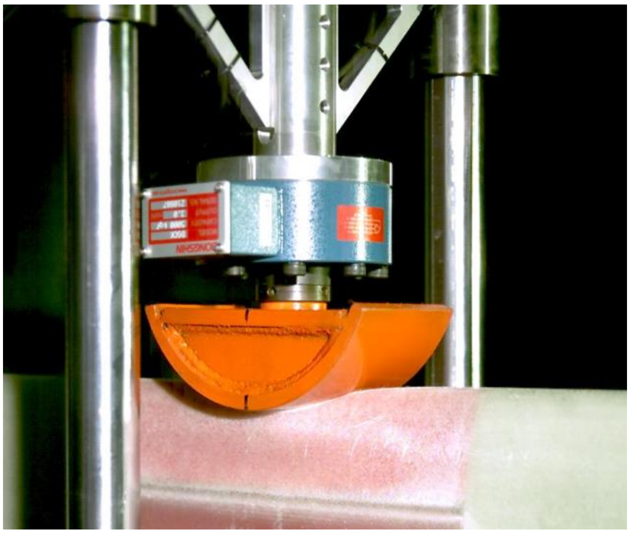

(b) Second test specimen

Figure 11: Rotor blades during maximum indentation

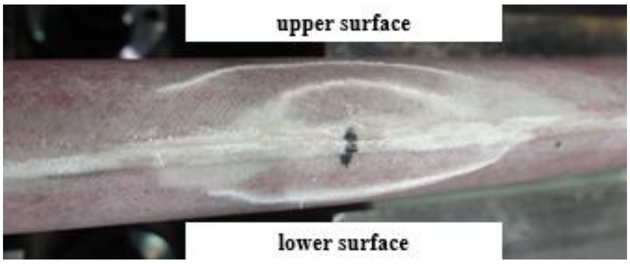

(a) First test specimen

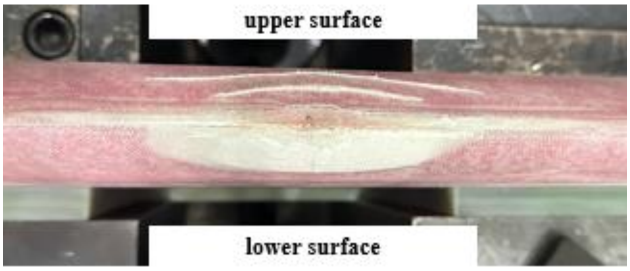

(b) Second test specimen

Figure 12: Rotor blades after crash impact

Force and displacement are set as 0 when the impact force rises significantly to compare between the test results. As shown in Fig. 13 (a), it is observed that extremely similar amount of total impact energies are applied on the rotor blades. However, different tendencies on the force curve are observed as shown in the red box in Fig. 13 (b) and (c). The impact force on the second test specimen results in a large extent of damage and the force curve is risen to a certain amount. However, relatively local damage occurs below the impactor of the first test specimen. This phenomenon is ascribed to be the rotor blade being disenabled to absorb the impact energy resulting in more indent.

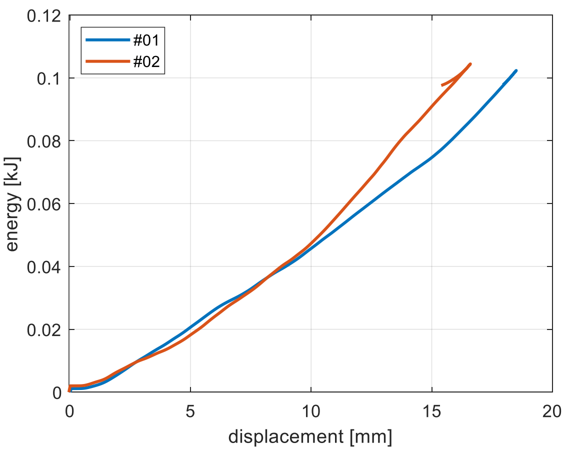

(a) Displacement- energy curve

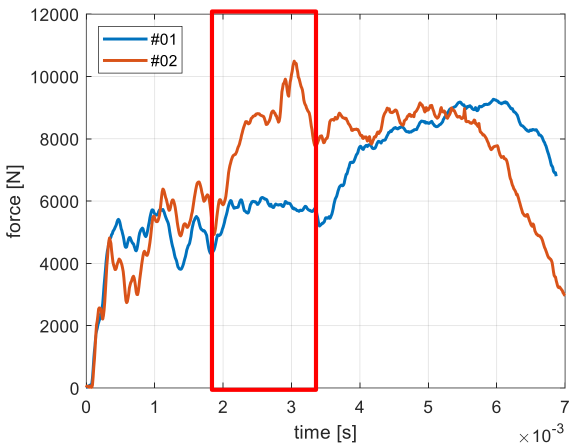

(b) Time-force curve

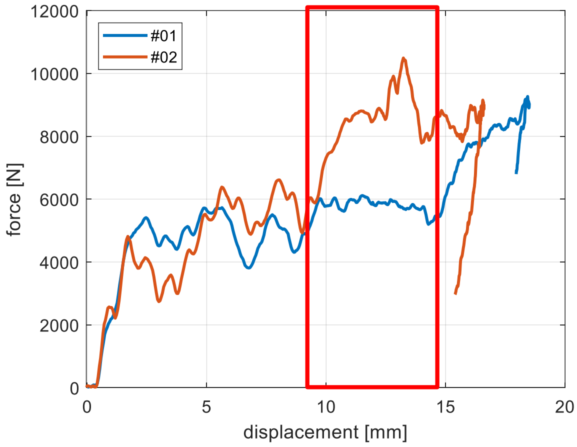

(c) Displacement- force curve

Figure 13: Experimental results of drop tests

4. ROTOR WHIRL TOWER TEST

4.1. Rotor blade and hub design

To simulate the hub loads of UH-60A and analyze the interaction of the load transferred to the hub, fan plot will be constructed by DYMORE as shown in Fig. 8. The information such as the experimental result of the rotor blade and configurations of flap/lag hinge, pitch bearing, pitch link and pitch horn are based on Refs. 13 and 16. Missing information such as the pitch link stiffness is adjusted to correlate the modal frequencies described in Ref. 14.

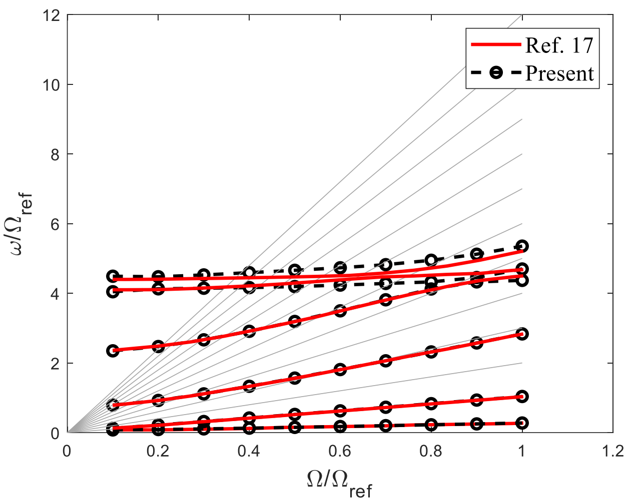

Figure 14: Full-scale rotor blade fan plot

Mach-scaled rotor blade and articulated hub are designed using the following information. The diameter of the small-scale rotor blade is set to be 2.5m, which brings the scale factor of 0.153. The dimension of the hub components is designed according to the scale factor. Furthermore, first torsion modal frequency becomes constant over pitch link stiffness if it is high enough. Therefore, the pitch link stiffness is designed to have high stiffness so that the manufacturing variability do not affect the modal frequency.

To correlate the modal frequencies of full-scale UH-60 rotor blade within certain discrepancy, cross section design of the rotor blade is selected as design variables. Accordingly, the structural properties of the small-scale rotor blade cross sections are evaluated using VABS program. Furthermore, the sectional properties evaluated by VABS are provided into DYMORE. Finally, MATLAB is used to analyze the modal frequencies to be within allowable tolerance when compared to those of a full-scale rotor blade. Figure 15 shows the procedure for designing the small-scale rotor blade for the whirl tower test.

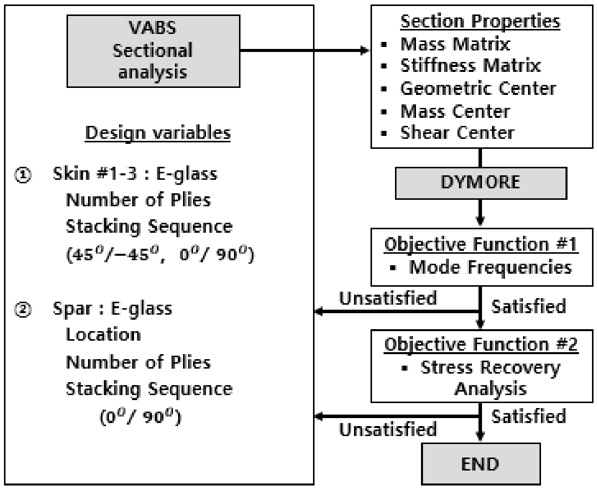

Figure 15: Design procedure for the small-scale rotor blade

The present design of the Mach-scaled UH60A rotor blade is shown in Fig. 16. The rotor blade is divided into 3 parts so that different layups of E-glass are applied along the chord. Furthermore, it consists of a E-glass spar, trailing edge filling and foam core.

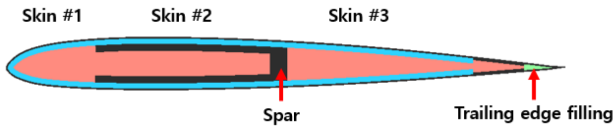

Figure 16: Presently designed rotor blade cross section for the whirl tower test

Five modal frequencies along with non-dimensionalized rotor speed are correlated within certain discrepancies as shown in Fig. 17. The modal frequencies are 1st lag, 1st flap, 2nd flap, 2nd lag and 1st torsion mode each from the bottom.

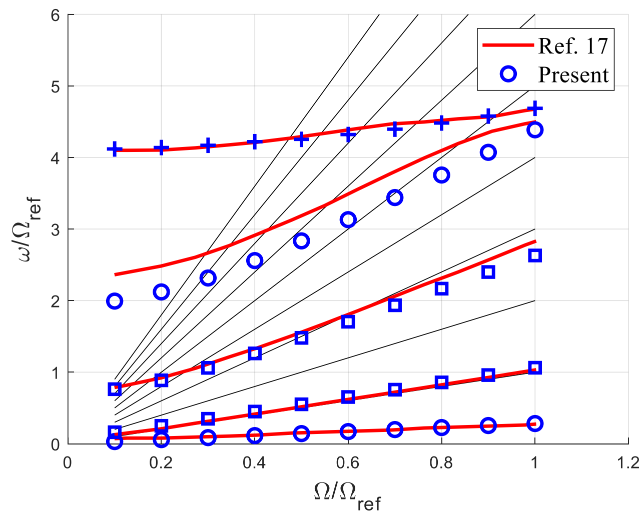

Figure 17: Small-scale rotor blade fan plot

4.2. Experimental and numerical evaluation

Whirl tower test will be conducted by using SNURTS and the rotor blade designed in Sec. 4.1. SNURTS is fabricated to experiment Seoul National University Flap (SNUF) blade equipped with an active trailing-edge flap as shown in Fig. 18[18]. Hover test will be conducted. In addition, to simulate the condition after the crash, one-blade-out hover test will be conducted. Finally, the loads acting on the hub will be measured and the correlation against the numerical analysis will be conducted.

Figure 18: Whirl tower test facility

5. CONCLUSIONS

1. In this paper, experimental and numerical evaluation of composite rotor blades under the crash is presented.
2. The rotor blades are designed to have the correct characteristics with UH-60A for each purpose of drop and whirl tower test.
3. Drop test is designed in accordance with MIL-STD 1290A and it is conducted to evaluate the maximum indentation and impact force during the crash impact. In addition, numerical evaluation is conducted and the correlation against the experimental result is investigated.
4. The design for Mach-scaled UH-60A rotor blade and hub is conducted to correlate the modal frequencies of the full-scale ones. Whirl tower test including the hover and one-blade-out hover test is to be conducted using SNURTS and the correlation between the experimental and numerical result will be investigated.

Author contact:

Changbae Lee lcb_109@snu.ac.kr

Kunhyuk Kong drkong123@snu.ac.kr

Seung-Hoon Kang shkang94@snu.ac.kr

Minho Hwang hmh2989@snu.ac.kr

SangJoon Shin ssjoon@snu.ac.kr

6. ACKNOWLEDGMENTS

The authors would like to acknowledge the financial support provided by the Defense Rapid Acquisition Technology Research Institute (DRATRI) of Korea (Project code 912849501).

7. REFERENCES

1. Anonymous, “Military Standard Light Fixed and Rotary-Wing Aircraft Crash Resistance,“ Department of Defense of USA, Washington, MIL-STD-1290A, 1988.
2. Park, I. K., Lim, J. S., Kim, S. J., and Kim, T. U., “Development and Assessment of Crashworthy Composite Subfloor for Rotorcrafts,” *Journal of the Korean Society for Aeronautical and Space Sciences*, Vol. 46, (1), 2018, pp. 18-31.
3. Jackson K. E., Boitnott R. L., Fasanella E. L., Jones, L. E., and Lyle, K. H., “A History of Full-Scale Aircraft and Rotorcraft Crash Testing and Simulation at NASA Langley Research Center,“ 4th Triennial International Aircraft and Cabin Safety Research Conference, Lisbon, Portugal, Nov. 2004.
4. Bolukbasi, A., et al., “Full Spectrum Crashworthiness Criteria for Rotorcraft,“ RDECOM-TR-12-D-12, 2011.
5. McCarthy, M. A., and Wiggenraad, J. F. M., “Numerical investigation of a crash test of a

composite helicopter subfloor structure, Composite Structures, Vol. 51, (4), 2001, pp.345-359.

6. Jackson, K. E., Fasanella, E. L., Boitnott, R. B., "Full-Scale Crash Test and Finite Element Simulation of a Composite Prototype Helicopter," NASA/TP-2003-212641, 2003.

7. Gupta, B. P., "Helicopter Obstacle Strike Tolerance Concepts Analysis," USARTL-TR-78-46, 1979.

8. Paek, S. K., and Han, J. H., "An Analysis Model Development for the Wood Impact Simulation of a Composite Rotor Blade," 1st Asian Australian Rotorcraft Forum and Exhibition, Busan, Korea, Feb. 2012.

9. Memon, W. A., Owen, I., and White, M. D., "Motion Fidelity Requirements for Helicopter-Ship Operations in Maritime Rotorcraft Flight Simulators," *Journal of Aircraft*, Vol. 56, (6), 2019, pp. 2189-2209.

10. Anonymous, "LS-DYNA Theory Manual; Release 10.0," Livermore Software Technology Corporation, Livermore, 2017.

11. Bousman, W. G., "Aerodynamic Characteristics of SC1095 and SC1094R8 Airfoils", NASA/TP-2003- 212265, 2003.

12. Yallaly, B., "Corn Hybrid Polymer Media for Coatings Removal from Delicate Substrates", JSEM Conference, May 2008.

13. Davis, S. J., "Predesign Study for a Modern 4-Bladed Rotor for RSRA," NASA-CR-166155, 1981.

14. Yu, W., Hodges, D. H. and Ho, J. C., "Variational Asymptotic Beam Sectional Analysis- An Updated Version," *International Journal of Engineering Science*, Vol. 59, 2012, pp. 40-64.

15. Yu, W., "VABS Manual for users," Utah State University, Logan, Utah, 2011.

16. Rex, W., Pflumm, T., and Hajek, M., "UH-60A Rotor and Coupled Rotor-Fuselage Simulation Framework Validation and Analysis," 45th European Rotorcraft Forum, Warsaw, Sep. 2019.

17. Yeo, H., and Potsdam, M., "Rotor Structural Loads Analysis Using Coupled Computational Fluid Dynamics/Computational Structural Dynamics," *Journal of Aircraft*, Vol. 53,(1), 2016, pp. 87-105.

18. Im, B. U., Lee, C. B., Eun, W. J., and Shin, S. J., "System Identification of SNUF Blade Equipped with an Active Trailing-Edge Flap," The 7th Asian/Australian Rotorcraft Forum, Jeju Island, Korea, October, 2018.